

# Replica symmetry breaking in trajectories of a driven Brownian particle

Masahiko Ueda<sup>1,\*</sup> and Shin-ichi Sasa<sup>1,†</sup>

<sup>1</sup>*Department of Physics, Kyoto University, Kyoto 606-8502, Japan*

(Dated: December 7, 2024)

We study a Brownian particle passively driven by a field obeying the noisy Burgers equation. We demonstrate that the system exhibits replica symmetry breaking in the path ensemble with the initial position of the particle fixed. The key step of the proof is that the path ensemble with a modified boundary condition can be exactly mapped to the canonical ensemble of directed polymers.

PACS numbers: 05.40.-a, 05.70.Fh, 64.70.P-

*Introduction.*— There exists a class of systems that exhibit *stable and diverse dynamics*. As a typical example of such dynamical behavior, one can consider cell differentiation, in which the self-replication of stem cells occurs robustly with the production of various types of cells [1, 2]. More generally, the concept of stable and diverse dynamics means that an observed time series is stable against perturbation like limit cycle, while a variety of trajectories are observed like chaos and Brownian motion. A natural question arising here is how stability and diversity are compatible, and an answer to this rather general question may shed light on the emergence of biological functions. However, our knowledge of stable and diverse dynamics is limited: for example, simple mathematical models of such dynamical behavior have not yet been proposed, because biological systems are too complicated. In this Letter, putting aside phenomena observed in biological systems, we study physical systems in which stable and diverse dynamics is observed.

For a state space endowed with probability, the stability of state can be characterized by the local maximality of the probability. Then, stable and diverse states are described by a rugged probability landscape, in which observed states may be condensed to one of several particular states. According to equilibrium statistical mechanics for mean-field spin glass models, such a phase is characterized by replica symmetry breaking (RSB) [3]. Now, we expect that stable and diverse dynamics, which is the focus of this Letter, can be characterized by extending the concept of RSB in state spaces to path spaces. More explicitly, when the probability in a path space has a rugged landscape, the observed trajectories are condensed to one of several particular trajectories.

To identify this phenomenon, we employ a method for detecting RSB in equilibrium statistical mechanics. Here, we review a quantity called *overlap*, which plays an essential role in the detection of RSB, by considering spin glass models as examples. Suppose that two independent and identical systems (replicas) are prepared. Then, the overlap represents the correlation of two spin variables at the same site. For sufficiently high temperatures, the overlap is expected to be zero because of the independence of the two systems. However, for temperatures

lower than some critical temperature, the overlap is not zero if both systems freeze in the same configuration, although it is zero when each system freezes to a different configuration, respectively. As a result, the distribution function of the overlap takes a non-trivial form. This corresponds to RSB.

We consider the overlap between trajectories in order to detect RSB in a path space with probability (path ensemble). Concretely, we prepare two independent and identical systems and define the overlap between the trajectories of both systems. We identify RSB by the existence of a non-trivial feature of the distribution function of the overlap. Here, it should be remarked that such an overlap has previously been considered for globally coupled maps exhibiting dynamical glasses [4, 5]. In these studies, the time average of the overlap of the instantaneous configurations was discussed, but this is not the same as a case in which a non-trivial overlap appears only when long-time trajectories are considered.

In this Letter, we present a simple model exhibiting RSB in trajectories of a single particle. Concretely, this model describes the dynamics of a Brownian particle passively driven by a field obeying the noisy Burgers equation [6]. We find that the overlap between trajectories obeys a non-trivial distribution and we then provide evidence to support the claim that this model exhibits RSB in the path ensemble.

*Model.*— Let  $x(t)$  be the one-dimensional position of a Brownian particle at time  $t \in [0, \tau]$ . The particle is assumed to be passively driven by a velocity field  $u(x, t)$ . The motion of the particle is then written as

$$\dot{x}(t) = u(x(t), t) + \xi(t), \quad (1)$$

where  $\dot{x}(t) \equiv dx(t)/dt$  and  $\xi(t)$  represents the thermal noise satisfying  $\langle \xi(t)\xi(t') \rangle = 2D\delta(t - t')$ .  $D$  is a diffusion constant for the free particle. The velocity field is assumed to obey the noisy Burgers equation. By setting  $u = -\partial\phi/\partial x$ , the equation for  $\phi$  is expressed as

$$\frac{\partial\phi}{\partial t} = \nu \frac{\partial^2\phi}{\partial x^2} + \frac{1}{2} \left( \frac{\partial\phi}{\partial x} \right)^2 + v(x, t). \quad (2)$$

This is called the Kardar-Parisi-Zhang (KPZ) equation [7], which has been studied extensively [8–16]. Here,

$v(x, t)$  is zero-mean Gaussian white noise with variance  $\langle v(x, t)v(x', t') \rangle = 2B\delta(x - x')\delta(t - t')$ . More precisely, since the space-time Gaussian white noise is not properly defined, it is necessary to introduce a cut-off length  $\Delta x$  in the space coordinate [16, 17]. Hereafter, we assume that all quantities are made dimensionless. We set  $\Delta x = 0.5$  and the derivatives in  $x$  that appear in (2) are interpreted as simple differences. Accordingly, the  $u$  acting on the particle is evaluated by linear interpolation of  $\phi$ . For completeness, we also note the domain of the particle position and the KPZ field. They are defined in a finite region with length  $L$  under periodic boundary conditions, and  $L$  is assumed to be sufficiently large.

Before presenting our results, we briefly review previous studies involving this model. It has been examined as an example of scalar turbulence [18], and it exhibits the remarkable phenomenon that non-interacting particles passively driven by the field cluster with time, where coalescence of valleys of the KPZ surface over time plays a key role [19]. Theoretically, renormalization group analysis has been performed [20]. Furthermore, the clusterization in the steady state was detected by studying density-density correlation functions [21, 22]. These previous studies indicate that particles in this model show a tendency towards localization. However, to the best of our knowledge, RSB in the path ensemble has never been reported.

*Numerical Result.*— We first present the numerical simulation results of the model. In particular, we focus on the  $D = \nu$  case, which corresponds to a fixed point of the renormalization group [20, 23]. Time integration is performed by employing the simplest discretization method with  $\Delta t = 0.01$ . We fix the initial position of the particle as  $x(0) = L/2$  with  $L = 10000$ . The initial value of the field,  $u(x, 0)$ , is sampled from the statistical steady state of (2). The parameter values are fixed as  $D = \nu = 1.0$  and  $B = 2.5$ . Here, it should be noted that there are two sources of randomness,  $\xi(t)$  and  $v(x, t)$ . In calculating an ensemble average of physical quantities, we first take the statistical average over  $N_1$  histories of noise  $\xi$  for one realization of  $u(x, t)$ , and then consider the configurational average over  $N_2$  realizations of  $v$ . The convergence of quantities with respect to the choice of  $(N_1, N_2)$  is carefully checked, and the numerical data presented below are obtained for  $N_1 = 80000$  and  $N_2 = 1000$ .

We start with observation of the trajectories for one realization of  $u(x, t)$ , which is displayed in Fig. 1. Each has the features of a typical trajectory of Brownian motion, while there exists a region in which several trajectories are overlapped. We shall quantify this observation.

First, on the left side of Fig. 2, the mean squared displacement of  $\sigma \equiv |x(t) - x(0)|$  as a function of  $t$  is displayed. The graph is deviated from the normal diffusion type, and the anomalous diffusion  $\langle \sigma^2 \rangle \simeq t^{4/3}$  is observed in the long time regime, as discussed in Refs. [19, 20]. A distribution of  $\sigma$  is also shown on the right

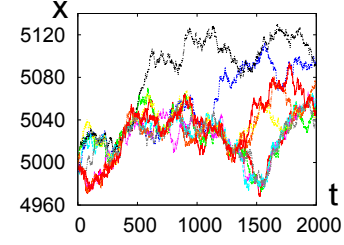


FIG. 1: (color online). Trajectories of a Brownian particle for one realization of  $u(x, t)$ . Ten samples are displayed.

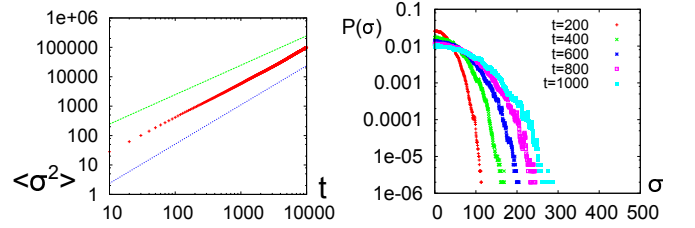


FIG. 2: (color online). The left figure shows the mean squared displacement  $\langle \sigma^2 \rangle$  as a function of  $t$  in a log-log plot. The straight lines represent the normal diffusion behavior  $\langle \sigma^2 \rangle \simeq t$  and the anomalous diffusion behavior  $\langle \sigma^2 \rangle \simeq t^{4/3}$ , respectively. The right figure shows the distribution of  $\sigma$  for various values of  $t$ . A logarithmic scale is used for the vertical axis. Throughout this Letter, we use the same symbols (and colors) for such distribution functions with the same  $t$ .

side of Fig. 2. As far as the one-particle behavior is concerned, nothing related to localization is observed.

Next, the mean squared value of relative distance  $d \equiv |x^{(1)} - x^{(2)}|$  for two trajectories  $x^{(1)}$  and  $x^{(2)}$  under the same  $u(x, t)$  is investigated. The normal relative diffusion behavior  $\langle d^2 \rangle \simeq t$  is clearly observed on the left side of Fig. 3. On the other hand, as shown on the right side of Fig. 3, the distribution of  $d$  at time  $t$ , which is denoted by  $P_t(d)$ , is far from the Gaussian distribution that is obtained for free Brownian particles. As a characteristic feature of  $P_t(d)$ , it is observed that the value of  $P_t(d)$  for  $d < 60$  does not change in time when  $t > 200$ . The existence of such a time-independent behavior means

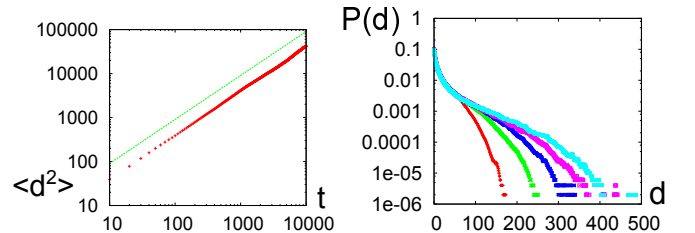


FIG. 3: (color online). The left figure shows the mean squared relative distance  $\langle d^2 \rangle$  as a function of  $t$  in a log-log plot. The straight line represents the normal diffusion behavior  $\langle d^2 \rangle \simeq t$ . The right figure shows the distribution of  $d$  for various values of  $t$ . A logarithmic scale is used for the vertical axis.

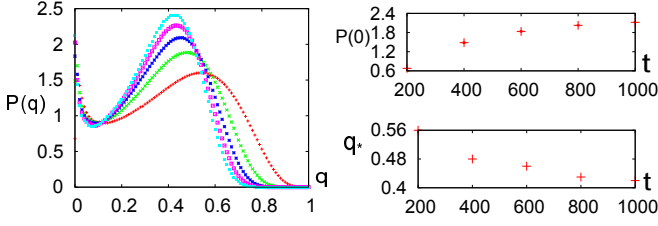


FIG. 4: (color online). Distribution of the overlap  $q$  for various  $t$  (left) and their peak values at  $q = 0$  and peak positions  $q_*(t)$  (right).

that the inter-distance of two particles is not significantly larger than a certain characteristic length. This provides one piece of quantitative evidence for a localization phenomenon. We estimated the characteristic length scale in this region as  $d_0 = 4.2$  [24]. Note that such a diffusion scaling with a non-Gaussian distribution has attracted considerable attention recently [25, 26].

Now, we consider the overlap defined by

$$q \equiv \frac{1}{M} \sum_{j=1}^M \theta \left( \ell - \left| x^{(1)}(j\Delta t) - x^{(2)}(j\Delta t) \right| \right), \quad (3)$$

for two trajectories  $x^{(1)}$  and  $x^{(2)}$  under the same  $u(x, t)$ . Here,  $M \equiv \tau/\Delta t$  and we have introduced the length scale  $\ell$  characterizing the localization. From the above discussion,  $\ell$  should be close to  $d_0$ . For simplicity, we set  $\ell = 5$ . On the left side of Fig. 4, we show the distribution function of the overlap,  $P(q)$ , for different values of  $\tau$ . There are two peaks at  $q = 0$  and  $q = q_*(\tau)$  for every  $\tau$ , which is a characteristic behavior observed in the one-step RSB (1RSB) [27]. The peak value at  $q = 0$  and the peak position  $q_*(\tau)$  are shown on the right side of Fig. 4. It seems that these approach finite values in the limit  $\tau \rightarrow \infty$ . In this Letter, we claim that RSB in the path ensemble occurs in the model under study, and we shall explain the reasoning below.

*Analysis.*— We present arguments to support this claim. A key observation is that the ensemble of trajectories of the particle under a modified boundary condition is equivalent to the canonical ensemble of directed polymers in random potentials with one end fixed. Explicitly, when we consider (1) and (2) with boundary conditions  $x(\tau) = x_0 = L/2$  and  $\phi(x, 0) = 0$ , the path probability density of the particle is written as

$$\mathcal{P}[x|x(\tau) = x_0] = \frac{1}{Z_{\text{DP}}} e^{-\frac{1}{4D} \int_0^\tau dt [\dot{x}(t)^2 - 2v(x(t), t)]}, \quad (4)$$

where  $Z_{\text{DP}}$  is the normalization constant. The proof is as follows. We first write the Onsager-Machlup expression of the path probability density as

$$\mathcal{P}[x|x(\tau) = x_0] = \frac{1}{Z_0} e^{-\frac{1}{4D} \int_0^\tau dt [\dot{x}(t) + \frac{\partial \phi}{\partial x}(x(t), t)]^2} \times e^{-\frac{1}{2} \int_0^\tau dt \frac{\partial^2 \phi}{\partial x^2}(x(t), t)}, \quad (5)$$

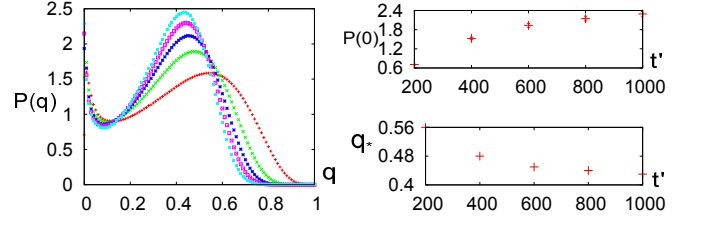


FIG. 5: (color online). Statistical properties of the ensemble (5). The distribution of the overlap,  $P(q)$ , for various  $t' \equiv \tau - t$  are plotted in the left side, and their peak values at  $q = 0$  and peak positions  $q_*(t')$  are displayed in the graph with  $t'$  in the right side. The symbols and color labels in the graph with  $t'$  are the same as those in the graph with  $t$  in Fig. 4

where  $Z_0$  is the normalization constant. We then rewrite (5) using (2) as

$$\begin{aligned} \mathcal{P}[x|x(\tau) = x_0] &= \frac{1}{Z_0} e^{-\frac{1}{4D} \int_0^\tau dt [\dot{x}(t)^2 + 2\frac{\partial \phi}{\partial x}(x(t), t) - 2\frac{\partial^2 \phi}{\partial x^2}(x(t), t)]} \\ &\quad \times e^{-\frac{1}{4D} \int_0^\tau dt \left\{ \left[ \frac{\partial \phi}{\partial x}(x(t), t) \right]^2 + 2D \frac{\partial^2 \phi}{\partial x^2}(x(t), t) \right\}}, \\ &= \frac{1}{Z_0} e^{-\frac{1}{2D} [\phi(x(\tau), \tau) - \phi(x(0), 0)] - \frac{1}{4D} \int_0^\tau dt [\dot{x}(t)^2 - 2v(x(t), t)]}, \\ &= \frac{1}{Z_0} e^{-\frac{1}{2D} \phi(x_0, \tau) - \frac{1}{4D} \int_0^\tau dt [\dot{x}(t)^2 - 2v(x(t), t)]}. \end{aligned} \quad (6)$$

Since the first term on the exponential can be absorbed into the normalization constant, we obtain (4).

The statistical model (4) has been extensively studied [16, 28–36], and it is known that the expectation of the overlap,  $\langle q \rangle$ , is non-zero for all parameter values [29]. Thus, this result shows that the Langevin model with the modified boundary condition exhibits RSB. If we are allowed to assume that the behavior in the time region  $1 \ll t \ll \tau$  is independent of boundary conditions, the original model can be shown to exhibit RSB. This is not a mathematical proof because the validity of the assumption of the boundary condition independence is not assured. Nevertheless, we can check the boundary condition dependence in numerical simulations. That is, we numerically investigate the modified system and compare the results with those obtained for the original model [37]. On the left side of Fig. 5, we show  $P(q)$  for the modified system. This is the almost same as that of the original case. The peak value and the non-trivial peak position also behave in the same way as the original model, as seen on the right side of Fig. 5. We are, therefore, confident that  $P(q)$  is independent of the boundary condition, and this implies that the original model surely exhibits RSB.

Here, we remark on the type of RSB. The numerical result for  $P(q)$  suggests 1RSB, because it contains two sharp peaks at  $q = 0$  and  $q = q_* \neq 0$ . However, it was pointed out that the replica symmetry of the model (4) is weakly broken [28, 29], which is in contrast to 1RSB

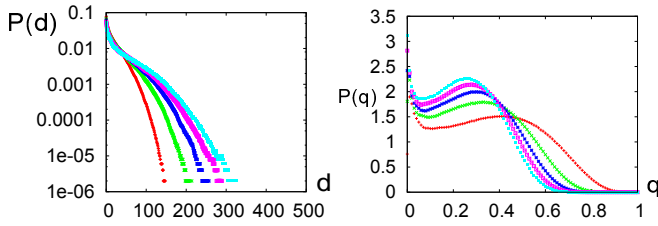


FIG. 6: (color online). Statistical quantities for a Brownian particle driven by a field obeying the EW equation. The distribution of the relative distance,  $P(d)$  (left), and the distribution of the overlap,  $P(q)$  (right).

or full RSB familiar in the theory of mean-field spin glass models. More precisely, while the free energy of the system is calculated from the replica symmetric ansatz, the expectation of the overlap between two identical copies coupled together with strength  $\epsilon$  experiences a jump at  $\epsilon = 0$  [38]. Furthermore, it was conjectured in Ref. [28] that  $P(q) = \delta(q - q_*)$  with  $q_* \neq 0$  in the limit  $\tau \rightarrow \infty$ , while the second peak of  $P(q)$  at  $q = 0$  for finite  $\tau$  shows slow relaxation of  $\tau^{-1/3}$  type. See Ref. [29] for a related argument. We also confirmed such slowly decaying behavior of the peak at  $q = 0$  for a discretized version of directed polymers [39]. This is qualitatively different from those in Figs. 4 and 5. Therefore, as far as we investigated, we cannot exclude a possibility of 1RSB for both the original model and the statistical model (5). Further numerical analysis will be required to settle this problem.

*Concluding Remarks.*— Before ending this Letter, we make three remarks related to the main result. First, as a control experiment, we study a passive particle driven by a field obeying the Edwards-Wilkinson (EW) equation [40]

$$\frac{\partial \phi}{\partial t}(x, t) = D \frac{\partial^2 \phi}{\partial x^2}(x, t) + v(x, t). \quad (7)$$

The distribution of the relative distance,  $P(d)$ , displayed on the left side of Fig. 6 exhibits non-Gaussian behavior, which is similar to the right side of Fig. 3. However, shape of the graph  $P(q)$  displayed on the right side of Fig. 6 is qualitatively different from that on the left side of Fig. 4, because the local minimum between the two  $P(q)$  peaks of Fig. 6 increases with time. Since the non-trivial peak would be absorbed into the peak at  $q = 0$  in the limit  $\tau \rightarrow \infty$ , we expect that there is no RSB for the EW case. As a related model, one may consider a particle system driven by the Gaussian random velocity field [41, 42], but we conjecture that there is no RSB at positive  $D$  in the model.

Second, one can regard RSB in the path ensemble as a dynamical transition characterized by the singularity of the *dynamical free energy* [43], which is the cumulant generating function of a time-averaged quantity. Indeed, the dynamical free energy associated with the overlap in our model exhibits a discontinuous transition when

the biasing parameter crosses over zero. Here, it should be recalled that the simplest example of such a dynamical phase transition was reported for the time-averaged activity of kinetically constrained models [44, 45]. The transition in this case corresponds to the standard first-order, while the transition in our case occurs only when two replicas are considered, similarly to the random first-order transition [46]. Thus, the present Letter provides another class of dynamical phase transitions.

The final remark is on the universality of the phenomenon. We expect that there are other systems that exhibit RSB in trajectories. One example may be a passive particle driven by a field obeying the Kuramoto-Sivashinsky equation [47, 48], which is a deterministic equation exhibiting spatio-temporal chaos [49]. Since its large-scale statistical properties may be described by the KPZ equation [50–55], RSB in the passive particle trajectories is expected to occur. Indeed, similarly to the KPZ equation case, a clustering phenomenon of non-interacting particles was observed [47], where the coalescence of attractive zeros of the velocity field was reported. Furthermore, with the coalescing paths, we associate the so-called Brownian web [56, 57]. As a totally different system, one may recall the Sinai model [58] that exhibits the Golosov localization [59], where the relative distance between two particles remains finite with probability one even in the infinite time limit. These systems will be studied in terms of RSB in trajectories in the future.

In sum, we have demonstrated RSB in trajectories for a particle passively driven by a field obeying the noisy Burgers equation. We believe that it is an important problem to deepen the understanding of the nature of this highly intriguing phenomenon. In particular, experimental observation of the phenomenon is quite challenging. We will also attempt to find similar phenomena in chemical networks in the future, which may be related to mechanisms of stable and diverse dynamics in biological systems.

The authors thank Takahiro Nemoto for useful discussions, especially on the derivation of (4). The present study was supported by KAKENHI (Nos. 25103002 and 26610115), a Grant-in-Aid for JSPS Fellows (No. 2681), and by the JSPS Core-to-Core program “Non-equilibrium dynamics of soft-matter and information.h

\* ueda@ton.scphys.kyoto-u.ac.jp

† sasa@scphys.kyoto-u.ac.jp

- [1] Z. S. Singer *et al.*, *Molecular cell* **55**, 319 (2014).
- [2] K. Kaneko, *Life: An Introduction to Complex Systems Biology* (Springer, New York, 2006).
- [3] M. Mézard, G. Parisi, and M. A. Virasoro, *Spin glass theory and beyond* (World Scientific, Singapore, 1987).
- [4] S. C. Manrubia and A. S. Mikhailov, *Europhys. Lett.* **53**, 451 (2001).

- [5] S. C. Manrubia, U. Bastolla, and A. S. Mikhailov, Eur. Phys. J. B **23**, 497 (2001).
- [6] J. Bec and K. Khanin, Physics Reports **447**, 1 (2007).
- [7] M. Kardar, G. Parisi, and Y.-C. Zhang, Phys. Rev. Lett. **56**, 889 (1986).
- [8] D. Forster, D.R. Nelson, and M.J. Stephen, Phys. Rev. A **16**, 732 (1977).
- [9] E. Medina, T. Hwa, M. Kardar, and Y.-C. Zhang, Phys. Rev. A **39**, 3053 (1989).
- [10] J. Krug, P. Meakin, and T. Halpin-Healy, Phys. Rev. A **45**, 638 (1992).
- [11] J. P. Bouchaud, M. Mézard, and G. Parisi, Phys. Rev. E **52**, 3656 (1995).
- [12] L. Bertini and G. Giacomin, Commun. Math. Phys. **183**, 571 (1997).
- [13] L. Canet, H. Chaté, B. Delamotte, and N. Wschebor, Phys. Rev. Lett. **104**, 150601 (2010).
- [14] T. Sasamoto and H. Spohn, Phys. Rev. Lett. **104**, 230602 (2010).
- [15] P. Calabrese and P. Le Doussal, Phys. Rev. Lett. **106**, 250603 (2011).
- [16] T. Halpin-Healy and Y.-C. Zhang, Physics Reports **254**, 215 (1995).
- [17] Y.-C. Zhang, Physica A **170**, 1 (1990).
- [18] B. I. Shraiman and E. D. Siggia, Nature **405**, 639 (2000).
- [19] C.-S. Chin, Phys. Rev. E **66**, 021104 (2002).
- [20] B. Drossel and M. Kardar, Phys. Rev. B **66**, 195414 (2002).
- [21] A. Nagar, M. Barma, and S. N. Majumdar, Phys. Rev. Lett. **94**, 240601 (2005).
- [22] A. Nagar, S. N. Majumdar, and M. Barma, Phys. Rev. E **74**, 021124 (2006).
- [23] D. Ertas and M. Kardar, Phys. Rev. E **48**, 1228 (1993).
- [24] See Supplemental Material at [URL will be inserted by publisher] for the estimation of the length scale.
- [25] B. Wang, S. M. Anthony, S. C. Bae, and S. Granick, Proc. Nat. Acad. Sci. **106**, 15160 (2009).
- [26] B. Wang, J. Kuo, S. C. Bae, and S. Granick, Nature Materials **11**, 481 (2012).
- [27] M. Mézard and A. Montanari, *Information, Physics and Computation* (Oxford University Press, Oxford, 2009).
- [28] G. Parisi, J. Phys. France **51**, 1595 (1990).
- [29] M. Mézard, J. Phys. France **51**, 1831 (1990).
- [30] M. Kardar and Y.-C. Zhang, Phys. Rev. Lett. **58**, 2087 (1987).
- [31] M. Kardar, Nucl. Phys. B **290** [FS20], 582 (1987).
- [32] J. P. Bouchaud and H. Orland, J. Stat. Phys. **61**, 877 (1990).
- [33] T. Hwa and D. S. Fisher, Phys. Rev. B **49**, 3136 (1994).
- [34] H. Yoshino, J. Phys. A: Math. Gen. **29**, 1421 (1996).
- [35] É. Brunet and B. Derrida, Phys. Rev. E **61**, 6789 (2000).
- [36] P. Calabrese, P. Le Doussal, and A. Rosso, Europhys. Lett. **90**, 20002 (2010).
- [37] See Supplemental Material at [URL will be inserted by publisher] for a numerical method for preparing the path ensemble (5).
- [38] See Supplemental Material at [URL will be inserted by publisher] for classification of RSB.
- [39] See Supplemental Material at [URL will be inserted by publisher] for numerical studies on the discretized version of directed polymers.
- [40] S. F. Edwards and D. R. Wilkinson, Proc. R. Soc. Lond. A **381**, 17 (1982).
- [41] J. M. Deutsch, J. Phys. A: Math. Gen. **18**, 1449 (1985).
- [42] M. Wilkinson and B. Mehlig, Phys. Rev. E **68**, 040101(R) (2003).
- [43] C. Beck and F. Schögl, *Thermodynamics of chaotic systems: an introduction* (Cambridge University Press, Cambridge, 1993).
- [44] J. P. Garrahan, R. L. Jack, V. Lecomte, E. Pitard, K. van Duijvendijk, and F. van Wijland, Phys. Rev. Lett. **98**, 195702 (2007).
- [45] J. P. Garrahan, R. L. Jack, V. Lecomte, E. Pitard, K. van Duijvendijk, and F. van Wijland, J. Phys. A: Math. Theor. **42**, 075007 (2009).
- [46] L. Berthier and G. Biroli, Rev. Mod. Phys. **83**, 587 (2011).
- [47] T. Bohr and A. Pikovsky, Phys. Rev. Lett. **70**, 2892 (1993).
- [48] X.-H. Wang and K.-L. Wang, Phys. Rev. E **49**, 5853 (1994).
- [49] Y. Kuramoto, *Chemical Oscillations, Waves, and Turbulence* (Springer, New York, 1984).
- [50] V. Yakhot, Phys. Rev. A **24**, 642 (1981).
- [51] S. Zaleski, Physica D **34**, 427 (1989).
- [52] K. Sneppen, J. Krug, M. H. Jensen, C. Jayaprakash, and T. Bohr, Phys. Rev. A **46**, R7351 (1992).
- [53] V. S. L'vov, V. V. Lebedev, M. Paton, and I. Procaccia, Nonlinearity **6**, 25 (1993).
- [54] F. Hayot, C. Jayaprakash, and C. Josserand, Phys. Rev. E **47**, 911 (1993).
- [55] C. C. Chow and T. Hwa, Physica D **84**, 494, (1995).
- [56] L. R. G. Fontes, M. Isopi, C. M. Newman, and K. Ravishanker, Proc. Nat. Acad. Sci. **99**, 15888 (2002).
- [57] B. Tsirelson, Lect. Notes Math. **1840** (2004).
- [58] Y. G. Sinai, Theory Probab. Appl. **27**(2), 256 (1982).
- [59] A. O. Golosov, Commun. Math. Phys. **92**, 491 (1984).

## SUPPLEMENTAL MATERIAL

### 1. Estimation of $d_0$

We estimate the characteristic length  $d_0$  of the time-independent region ( $t > 200$ ) of  $P(d)$  in Fig. 3 in the main text. Note that a logarithmic scale was used for the vertical axis. In Fig. S1,  $\log[P(d)/P(0)]$  is plotted as a function of  $d$ . We find two different behaviors: the exponential form in small  $d$  ( $d < 2$ )

$$\log \frac{P(d)}{P(0)} = -\frac{d}{d_0}, \quad (\text{S1})$$

and the stretched exponential form

$$\log \frac{P(d)}{P(0)} = -\left(\frac{d}{b}\right)^\alpha \quad (\text{S2})$$

in large  $d$  ( $20 < d < 60$ ). We interpret that two particles are trapped when their distance is less than  $d_0$ . We thus characterize the localization length by  $d_0$ . Two straight lines in Fig. S1 represent (S1) with  $d_0 = 4.2$  and (S2) with  $\alpha = 0.35$  and  $b = 1.7$ , respectively.

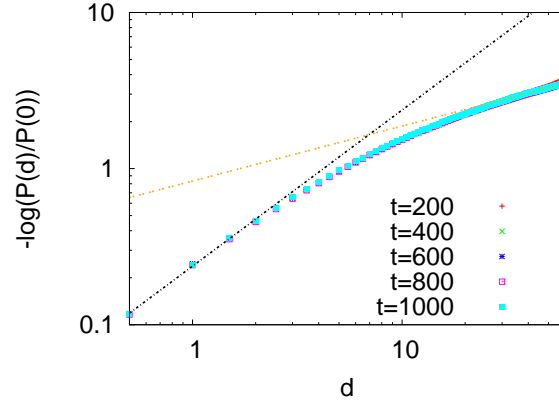


FIG. S1: (color online). A log-log plot of  $-\log[P(d)/P(0)]$  in the range  $d \in [0, 60]$ . The two straight lines represent (S1) with  $d_0 = 4.2$  and (S2) with  $\alpha = 0.35$  and  $b = 1.7$ , respectively.

### 2. Numerical realization of (5)

We explain a numerical method for obtaining the path ensemble given by (5) where the final condition  $x(\tau)$  is fixed. First, we calculate  $\phi(x, t)$ , which obeys the KPZ equation (2) with the initial condition  $\phi(x, 0) = 0$ , during a time interval  $t \in [0, \tau]$  and store the values of  $\phi(x, t)$  for all  $x$  and  $t$ . Then we calculate  $\tilde{x}(t) \equiv x(\tau - t)$  from the Langevin equation

$$\dot{\tilde{x}}(t) = \frac{\partial \phi}{\partial x}(\tilde{x}(t), \tau - t) + \xi(t) \quad (\text{S3})$$

with the fixed initial condition  $\tilde{x}(0) = x_0$ . The path probability density of  $\tilde{x}(t)$  is given by

$$\tilde{\mathcal{P}}[\tilde{x}|\tilde{x}(0) = x_0] = \frac{1}{Z_0} e^{-\frac{1}{4D} \int_0^\tau dt [\dot{\tilde{x}}(t) - \frac{\partial \phi}{\partial x}(\tilde{x}(t), \tau - t)]^2 - \frac{1}{2} \int_0^\tau dt \frac{\partial^2 \phi}{\partial x^2}(\tilde{x}(t), \tau - t)}, \quad (\text{S4})$$

which is indeed equal to (5) due to the definition  $\tilde{x}(t) = x(\tau - t)$ . In this way, we can construct the path ensemble (5).



### 3. Type of RSB

We briefly review classification of RSB. In general, RSB in a system is detected by the nontriviality of  $P(q)$ . The graph of  $P(q)$  in a RSB phase takes one of several forms [1]. For the full RSB case,  $P(q)$  is a broad function even in the limit  $\tau \rightarrow \infty$ . For the one-step RSB (1RSB) case,  $P(q)$  converges to a sum of two  $\delta$ -functions in the limit  $\tau \rightarrow \infty$ . In addition to these well-known cases, there is a case that  $\lim_{\tau \rightarrow \infty} P(q)$  has a single peak, but the replica symmetry of the system is broken in the sense that there are many metastable states whose free energy per one degree of freedom is equal to that of the lowest free energy state [2, 3]. This case is called a weak breaking of the replica symmetry [4, 5].

More explicitly, we can formulate and classify RSB by considering an  $\epsilon$ -biased ensemble with the biasing factor  $e^{\tau \epsilon q}$ . That is, by defining the scaled cumulant generating function

$$\psi(\epsilon) \equiv \lim_{\tau \rightarrow \infty} \frac{1}{\tau} \log \langle e^{\tau \epsilon q} \rangle, \quad (\text{S5})$$

we consider the expectation of the overlap in the  $\epsilon$ -biased ensemble

$$\langle q \rangle_\epsilon \equiv \frac{\partial}{\partial \epsilon} \psi(\epsilon). \quad (\text{S6})$$

We identify RSB if  $\lim_{\epsilon \rightarrow +0} \langle q \rangle_\epsilon \neq \lim_{\epsilon \rightarrow -0} \langle q \rangle_\epsilon$ . In particular, the overlap  $q$  in the 1RSB case, takes two values at  $\epsilon = 0$  depending on the limit  $\epsilon \rightarrow +0$  or  $\epsilon \rightarrow -0$ , while the overlap in the weak breaking case takes only one of them in the limit  $\tau \rightarrow \infty$ . See Fig. S2 as schematic graphs representing this fact.

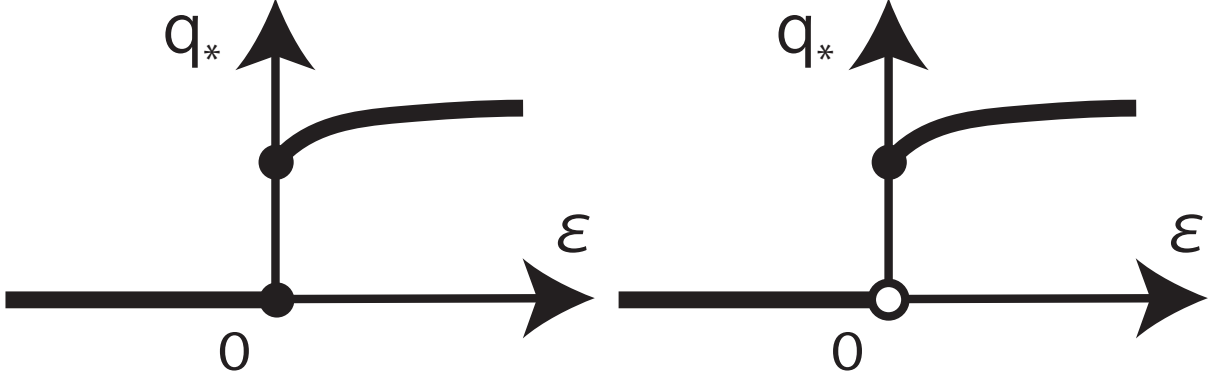


FIG. S2: Schematic graphs of the peak position  $q_*$  of  $P(q)$  for the 1RSB case (left) and the weak breaking case (right).

### 4. Discretized version of directed polymers

We provide numerical results for  $P(q)$  for a discretized version of directed polymers. We consider a polymer on the square lattice as a path  $[y] \equiv (y_0, y_1, \dots, y_M)$  with  $y_j \in \{1, \dots, N\}$  satisfying the constraint  $y_{j+1} \in \{y_j - 1, y_j, y_j + 1\}$ . The periodic boundary conditions are used in the  $y$  direction. The polymer is subjected to a zero mean Gaussian random potential  $v(y, j)$  with variance  $\langle v(y, j)v(y', j') \rangle = A\delta_{y,y'}\delta_{j,j'}$ . We assume the following equilibrium distribution of the polymer with one end fixed:

$$\mathcal{P}_{\text{DP}}[y|y_0 = a] = \frac{1}{Z} \prod_{j=0}^{M-1} e^{-v(y_{j+1}, j+1)} [\delta_{y_{j+1}, y_j} + \gamma \delta_{y_{j+1}, y_j+1} + \gamma \delta_{y_{j+1}, y_j-1}], \quad (\text{S7})$$

where  $Z$  is the normalization constant and  $\gamma$  is a parameter related to an elastic constant [5]. The partition function  $Z$  of this model was calculated by using a method of the transfer matrix [6]

$$Z(y, j+1) = \sum_{y'} T_{j+1}(y|y') Z(y', j), \quad (\text{S8})$$

$$T_{j+1}(y|y') \equiv \frac{1}{1+2\gamma} e^{-v(y, j+1)} [\delta_{y, y'} + \gamma \delta_{y, y'+1} + \gamma \delta_{y, y'-1}] \quad (\text{S9})$$

with the initial condition  $Z(y, 0) = \delta_{y,a}$ .

We define the overlap between two trajectories  $[y^{(1)}]$  and  $[y^{(2)}]$  as

$$q\left([y^{(1)}], [y^{(2)}]\right) \equiv \frac{1}{M} \sum_{j=1}^M \delta_{y_j^{(1)}, y_j^{(2)}}. \quad (\text{S10})$$

The distribution of the overlap  $P(q)$  for this model was measured numerically. The parameter values used in the calculation are  $A = 1.0$  and  $\gamma = 0.1$ . The statistical average was taken over 80000 samples for one fixed realization of the potential, and the disorder average with respect to random potentials was calculated from 2000 samples. The result is shown on the left side of Fig. S3. Two peaks are observed similarly to those in the main text, but the important difference is that, as shown on the right side of Fig. S3, the peak at  $q = 0$  decreases as a power law function  $\tau^{-\mu}$ , which is consistent with the prediction in Refs. [4, 5]. More precisely, although the value of  $\mu$  estimated from the numerical data is closer to  $1/4$  than  $1/3$  proposed in previous studies [4, 5], we conjecture that this slight discrepancy comes from finite size effects. It should be noted that the increasing behavior of  $P(q = 0)$  on the right side of Fig. 5 in the main text has never been observed in this model.

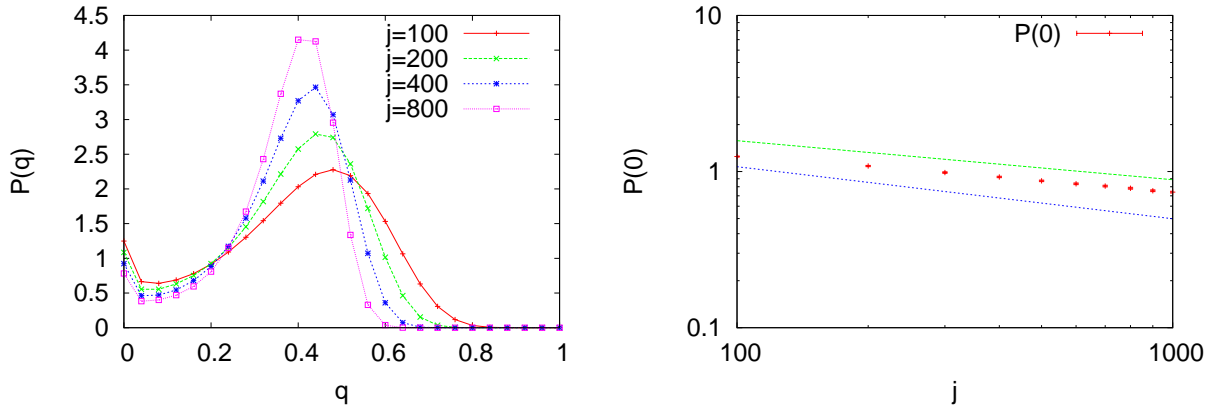


FIG. S3: (color online). The left figure shows the overlap distribution  $P(q)$  for the discretized model. The right figure shows the time dependence of  $P(q = 0)$  in a log-log plot. The two straight lines represent  $P(0) \simeq j^{-1/4}$  and  $P(0) \simeq j^{-1/3}$ , respectively.

For completeness, we explain our calculation method of  $P(q)$ , which relies on a Markov chain model whose path probability is equivalent to (S7). Below, we shall explain the Markov chain explicitly.

We construct a Markov chain by extending a method proposed in Refs. [7, 8] to that for time-dependent cases [9]. First, we define a function  $\Phi(y, j)$  by an equation

$$\Phi(y', j) = \sum_y \Phi(y, j+1) T_{j+1}(y|y') \quad (\text{S11})$$

with the final condition  $\Phi(y, M) = 1$ . Next, by defining

$$\tilde{T}_{j+1}(y|y') \equiv \frac{\Phi(y, j+1)}{\Phi(y', j)} T_{j+1}(y|y'), \quad (\text{S12})$$

we can confirm  $\sum_y \tilde{T}_{j+1}(y|y') = 1$  from the definition of  $\Phi$ . Thus, by identifying  $\tilde{T}$  as a time dependent transition probability, we have a Markov chain

$$P(y, j+1) = \sum_{y'} \tilde{T}_{j+1}(y|y') P(y', j). \quad (\text{S13})$$

We fix the initial condition as  $P(y, 0) = \delta_{y,a}$  with some  $a$ .

Now, we write a realization of state at time  $j$  as  $y_j$  and denote a path by  $[y] \equiv (y_0, y_1, \dots, y_M)$ . The probability of path is given by

$$\mathcal{P}[y|y_0 = a] \equiv \prod_{j=0}^{M-1} \tilde{T}_{j+1}(y_{j+1}|y_j). \quad (\text{S14})$$



This can be rewritten as

$$\begin{aligned}
\mathcal{P}[y|y_0 = a] &= \frac{\Phi(y_M, M)}{\Phi(y_0, 0)} \prod_{j=0}^{M-1} T_{j+1}(y_{j+1}|y_j) \\
&= \frac{1}{\Phi(a, 0)} \prod_{j=0}^{M-1} T_{j+1}(y_{j+1}|y_j) \\
&= \frac{1}{Z} \prod_{j=0}^{M-1} e^{-v(y_{j+1}, j+1)} [\delta_{y_{j+1}, y_j} + \gamma \delta_{y_{j+1}, y_{j+1}} + \gamma \delta_{y_{j+1}, y_{j-1}}], \tag{S15}
\end{aligned}$$

where  $Z$  is the normalization constant. This path probability is equivalent to (S7). In numerical calculation,  $\Phi(y, j)$  is calculated by (S11), and then  $\mathcal{P}[y|y_0 = a]$  is obtained by (S14). By collecting trajectories numerically, we obtained  $P(q)$ .

---

\* ueda@ton.scphys.kyoto-u.ac.jp

† sasa@scphys.kyoto-u.ac.jp

- [1] M. Mézard and A. Montanari, *Information, Physics and Computation* (Oxford University Press, Oxford, 2009).
- [2] D. A. Huse and D. S. Fisher, J. Phys. A: Math. Gen. **20**, L997 (1987).
- [3] G. Parisi and M. A. Virasoro, J. Phys. France **50**, 3317 (1989).
- [4] G. Parisi, J. Phys. France **51**, 1595 (1990).
- [5] M. Mézard, J. Phys. France **51**, 1831 (1990).
- [6] T. Halpin-Healy and Y.-C. Zhang, Physics Reports **254**, 215 (1995).
- [7] R. L. Jack and P. Sollich, Prog. Theor. Phys. Supp. **184**, 304 (2010).
- [8] T. Nemoto and S.-i. Sasa, Phys. Rev. E **84**, 061113 (2011).
- [9] The construction method of such Markov processes for time-dependent cases was provided by T. Nemoto.